INTERNATIONAL JOURNAL OF AUTOMOTIVE AND MECHANICAL ENGINEERING
ISSN: 2229-8649 e-ISSN: 2180-1606
VOL. 21, ISSUE 3, 2024, 11663 – 11681
DOI: https://doi.org/10.15282/ijame.21.3.2024.17.0900

REVIEW ARTICLE

Integrated Chassis Control for Multi-Axle Vehicles: A Comprehensive Review

M.S.M. Zakaria[1,2], A.S.P. Singh[1,3]*, and M.S.M. Aras[4]

[1]Faculty of Mechanical Technology and Engineering, Universiti Teknikal Malaysia Melaka, 76100 Durian Tunggal, Melaka, Malaysia
[2]Automotive Engineering Division, Road Transport Department of Malaysia, Level 4, No. 26, Jalan Tun Hussein, Presint 4, 62100 Putrajaya, Malaysia
[3]Centre for Advanced Research on Energy, Universiti Teknikal Malaysia Melaka, 76100 Durian Tunggal, Melaka, Malaysia
[4]Faculty of Electrical Technology and Engineering, Universiti Teknikal Malaysia Melaka, 76100 Durian Tunggal, Melaka, Malaysia

ABSTRACT – Multi-axle vehicles (MAVs) are used to transport heavy loads, navigate challenging terrain, and perform specific tasks. However, designing vehicle control systems for such vehicles is challenging. MAVs, such as trucks, buses, military vehicles, and multi-purpose vehicles, require sophisticated control techniques to increase the stability and ride comfort of such vehicles. This paper provides a comprehensive review of standalone control systems and integrated control systems (ICSs) for the steering, driving/braking, and suspension systems of MAVs, with a particular focus on the optimal tyre force distribution (TFD) in ICSs for MAVs. It also discusses various objective functions and optimisation methods used for the TFD. The findings indicate that optimising TFD significantly improves the stability of MAVs. As such, future studies may consider examining optimising three-axis TFD for MAVs to further improve vehicle stability.

ARTICLE HISTORY
Received : 14th March 2024
Revised : 13th Aug. 2024
Accepted : 09th Sept. 2024
Published : 20th Sept. 2024

KEYWORDS
Integrated chassis control
Optimal tyre force distribution
Ride comfort
Trajectory tracking
Vehicle stability

1. INTRODUCTION

The concept of multi-axle vehicles (MAVs), including various types of vehicles such as trucks, buses, military vehicles, and multi-purpose vehicles, has significantly shaped the landscape of modern transportation. Unlike a two-axle vehicle, an MAV is purposely built to carry larger loads, navigate challenging terrain, and perform specialised tasks. These characteristics of MAVs have made the designing of vehicle control systems more challenging. Vehicle control systems can be categorised as standalone control systems (SCSs) and integrated control systems (ICSs). Standalone control systems (SCSs), which refer to individual control systems that operate independently, focus on specific functions in the performance of a vehicle [1]. Standalone control systems (SCSs) comprise the steering, driving/braking, and suspension control systems, where the steering system is developed to control the direction [2], the driving or braking system to improve the longitudinal performance [3, 4], and the semi-active suspension (SAS) or active suspension (AS) system to minimise ride discomfort [5, 6] of the vehicle. However, SCSs may have limitations compared to ICSs, which are becoming increasingly common in modern vehicles for improved vehicle stability and ride comfort.

The ICSs discussed in the present paper include the integrated control of the steering and wheel torque, suspension and wheel torque, and steering and suspension systems. Several studies have been undertaken on the use of integrated steering and wheel torque control systems to achieve improved vehicle stability and trajectory tracking [7–9]. In this type of integration, tyre forces are applied longitudinally and laterally to increase vehicle stability. The integration of suspension and wheel torque, as studied by Chen *et al.* [10] and Li *et al.* [11], improves vehicle performance and comfort, while integrated steering and suspension systems are designed to increase vehicle stability and comfort [12]. The use of the optimal tyre force distribution (TFD) in an ICS can further improve vehicle stability by preventing tyre force saturation. An optimal TFD minimises either tyre force usage [3, 13] or tyre workload [11, 14] to prevent the vehicle from becoming unstable. In other studies, the optimal TFD is used to minimise the dissipation of tyre energy [15, 16]. In these optimal distribution methods, tyre forces are allocated to achieve stability or reduce energy dissipation. The optimal three-axis TFD for MAVs, especially to extend vehicle stability, can be explored.

This paper is aimed at reviewing the control strategies for MAVs to enhance vehicle stability, trajectory tracking, and ride comfort. Both SCSs and ICSs will be reviewed in depth for steering, driving/braking, and suspension systems in MAVs, with a particular emphasis on the optimisation of the TFD within ICSs. This paper will also discuss various objective functions and optimisation methods for the TFD. The remainder of the present paper is organised as follows: Sections 2 and 3 present the vehicle dynamics and tyre models, respectively. The SCSs for steering, driving/braking, and suspension in MAVs are presented in Section 4. Section 5 presents the ICSs for these systems, and Section 6 discusses the methods for obtaining the optimal TFD. Section 7 presents the future direction for the optimisation of three-axis tyre forces in MAVs, while the conclusions are provided in Section 8.

***CORRESPONDING AUTHOR | A.S.P. Singh** | ✉ amriksingh@utem.edu.my

2. VEHICLE MODELLING

Vehicle modelling is a fundamental part of vehicle dynamics control as it plays an essential role in understanding and simulating the dynamic behaviour of MAVs. This section introduces the various vehicle models used in this field of study. A summary of three- and four-axle vehicle models is included in Tables 1 and 2, respectively.

Table 1. Two-degrees-of-freedom (2-DOF), 3-DOF, 9-DOF, 18-DOF, and 24-DOF models for three-axle vehicles

DOF	Motion	Reference
2	Vehicle body: lateral and yaw	[11, 17–29]
3	Vehicle body: longitudinal, lateral, and yaw	[30, 31]
9	Handling model Vehicle body: longitudinal, lateral, and yaw Wheel: rotational	[32–35]
	Ride model Vehicle body: vertical, pitch, and roll Wheel: vertical	[36]
11	Vehicle body: lateral, vertical, yaw, pitch, and roll Wheel: vertical	[12]
18	Vehicle body: longitudinal, lateral, vertical, yaw, pitch and roll Wheel: rotational and vertical	[11, 17–20, 37–41]
24	Vehicle body: longitudinal, lateral, vertical, yaw, pitch and roll Wheel: rotational and vertical Steering: 6-DOF	[22, 42]

Table 2. 2-DOF, 3-DOF, 11-DOF, and 22-DOF models for four-axle vehicles

DOF	Motion	Reference
2	Vehicle body: lateral and yaw	[3, 9, 43–57]
3	Vehicle body: longitudinal, lateral, and yaw	[4]
11	Handling model Vehicle body: longitudinal, lateral, and yaw Wheel: rotational	[58–62]
	Ride model Vehicle body: vertical, pitch, and roll Wheel: vertical	[6, 63, 64]
22	Vehicle body: longitudinal, lateral, vertical, yaw, pitch, and roll Wheel: rotational and vertical	[46, 48, 65–68]

2.1 Three-Axle Vehicle Model

2.1.1 2 DOF vehicle model

Figure 1 depicts a simple 2-DOF vehicle model, which is useful for studying the dynamics of a vehicle's handling. This simple vehicle model comprises the lateral and yawing motions of a vehicle, which may be used to examine its handling characteristics. The steering angles at the front, middle, and rear axles, indicated by δ_f, δ_m, and δ_r, respectively, are used as the inputs for this model. The vehicle velocity along the longitudinal axis is assumed to be constant. In Eqs. (1) and (2), as well as Figure 1, F_{yi} is the lateral tyre force of axle i.

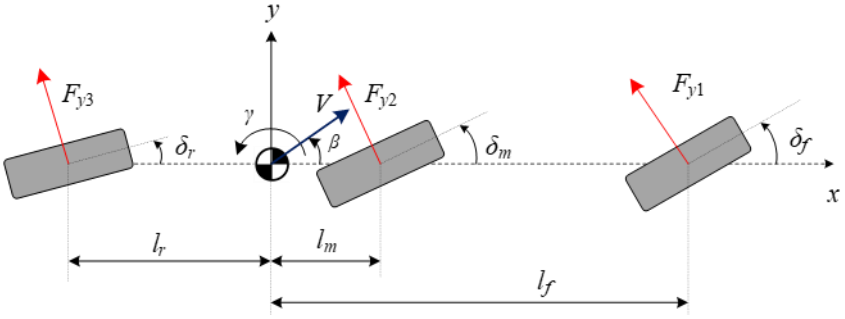

Figure 1. A 2-DOF vehicle model

The following two equations were used to set the lateral and yaw motions of a vehicle:

$$mV(\dot{\beta} + \gamma) = F_{y1}\cos\delta_f + F_{y2}\cos\delta_m + F_{y3}\cos\delta_r \quad (1)$$

$$I_Z\dot{\gamma} = l_f F_{y1}\cos\delta_f + l_m F_{y2}\cos\delta_m - l_r F_{y3}\cos\delta_r \quad (2)$$

where, β is the sideslip angle, γ is the yaw rate, m is the mass of the vehicle, and I_z is the moment of inertia for yaw.

2.1.2 9-DOF vehicle model

The 9-DOF vehicle models discussed here are often referred to as vehicle handling models. The 9-DOF model depicted in Figure 2 provides a more advanced and detailed mathematical representation of vehicle handling dynamics than a 2-DOF model. The steer angles and driving/braking wheel torque were used as inputs in the 9-DOF vehicle model. This model includes not only the longitudinal, lateral, and yawing motions of a vehicle but also the rotating motion of each wheel [32, 34].

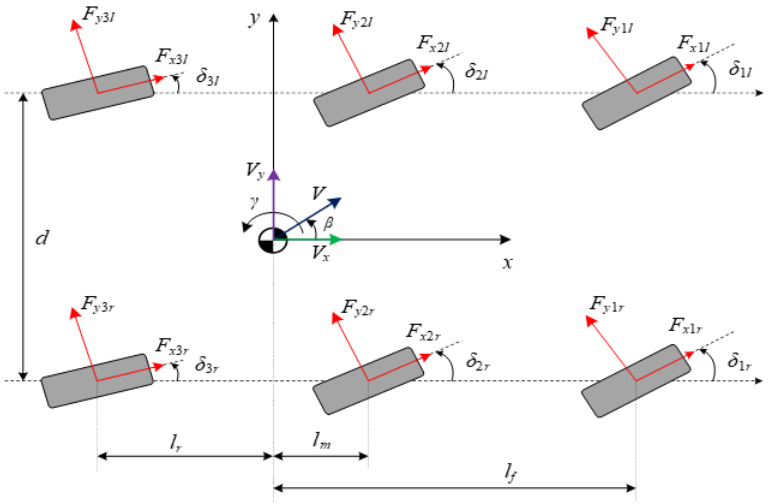

Figure 2. 9-DOF planar vehicle model

The steer angles of the first, second, and third axles are indicated by δ_{1l}, δ_{1r}, δ_{2l}, δ_{2r}, δ_{3l}, and δ_{3r}. The steer angles of both wheels on the same axle were considered to be identical. The longitudinal and lateral tyre forces are denoted by F_{xij} and F_{yij}, respectively. The subscripts i and j (i axle numbers = 1, 2, and 3) and (j, wheel positions = r, right, and l, left). Figure 3 provides a schematic of the wheel dynamics, where I_{wij} is the moment of inertia of the wheel, ω_{wij} is its rotational speed, T_{wij} is its torque, and r_{ij} is its radius.

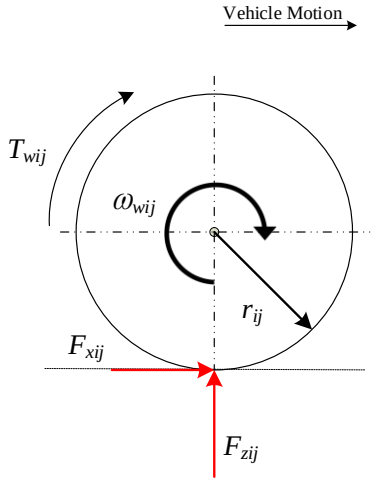

Figure 3. Schematic of the wheel dynamics

2.1.3 18-DOF vehicle model

The 18-DOF model depicted in Figure 4 includes the translational motions in the longitudinal, lateral, and vertical directions as well as the yawing, rolling, and pitching motions of the body of the vehicle and the rotating and vertical motions of its wheels. The steer angles, wheel torques, and elevation of the vertical road profile were all inputs to the 18-DOF model. For the first, second, and third axles, two wheels on the same axle were considered to have identical steer angles. In addition, the tyres were assumed to be in continuous contact with the ground. Similar models were used by Kim *et al.* [26] and Nah *et al.* [42], but with an added 6-DOF steering system.

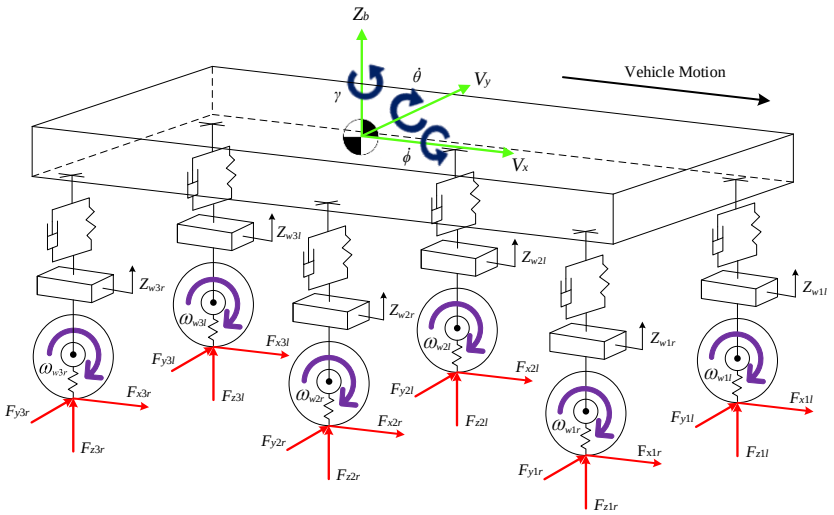

Figure 4. 18-DOF vehicle model

In Figure 4, the tyre longitudinal, lateral, and vertical forces are denoted as F_{xij}, F_{yij}, and F_{zij}, respectively, while the rolling angle, pitching angle, and yaw velocity are represented as ϕ, θ, and γ, respectively. Z_{wij} is the displacement of the wheel's mass, while ω_{wij} is its rotational speed.

2.2 Four-Axle Vehicle Model

2.2.1 2-DOF vehicle model

Figure 5 illustrates a single-track vehicle that has 2-DOF. The model considers the lateral and yawing motions of a vehicle. The first two axles were steerable and the steering angles of these axles, namely, δ_1 and δ_2, respectively, were used as inputs in the vehicle model. The speed of the vehicle was kept constant. In Figure 5, F_{yi} is the lateral tyre force, and i = 1, 2, 3, and 4, indicating the first, second, third, and fourth axles, respectively. The lateral and yaw equations of motion were written as follows:

$$mV(\dot{\beta} + \gamma) = F_{y1}\cos\delta_1 + F_{y2}\cos\delta_2 + F_{y3} + F_{y4} \tag{3}$$

$$I_Z\dot{\gamma} = l_1F_{y1}\cos\delta_1 + l_2F_{y2}\cos\delta_2 - l_3F_{y3} - l_4F_{y4} \tag{4}$$

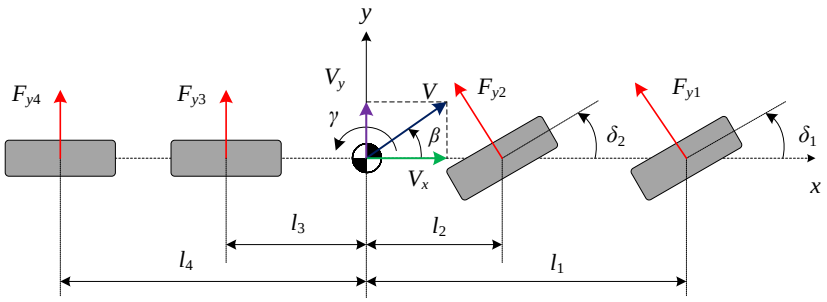

Figure 5. 2-DOF vehicle model

Each tyre in this single-track vehicle model represents two tyres on the same axle, and the black and white circle represents the centre of gravity (CG) of the vehicle. The CG is located between the second and third axles. The distances from the first, second, third, and fourth axles to the CG of the vehicle are given as l_1, l_2, l_3, and l_4, respectively. All these forces are depicted in red arrows.

2.2.2 11-DOF vehicle model

The 11-DOF vehicle models included in the present paper may be categorised as vehicle handling and ride models. Figure 6 presents an 11-DOF vehicle handling model. This vehicle handling model is more complex than a 2-DOF vehicle model because the 2-DOF model includes only lateral and yawing motions, while the 11-DOF model includes the longitudinal, lateral, and yawing motions of the body of the vehicle and the rotational motion of each wheel [59, 69]. The 11-DOF model assumes motion on the horizontal plane. The inputs in the 11-DOF handling model were the steer angles of the front two axles and the wheel torques of all the axles. The steer angles at the first and second axles are denoted by δ_{1l}, δ_{1r}, δ_{2l}, and δ_{2r}, respectively. For the front two axles, two wheels on each axle had the same steer angle. The tyre longitudinal and lateral forces are denoted by F_{xij} and F_{yij}, respectively. The subscripts i and j (i, axle number = 1, 2, 3 and 4) and (j, wheel position = r, right and l, left).

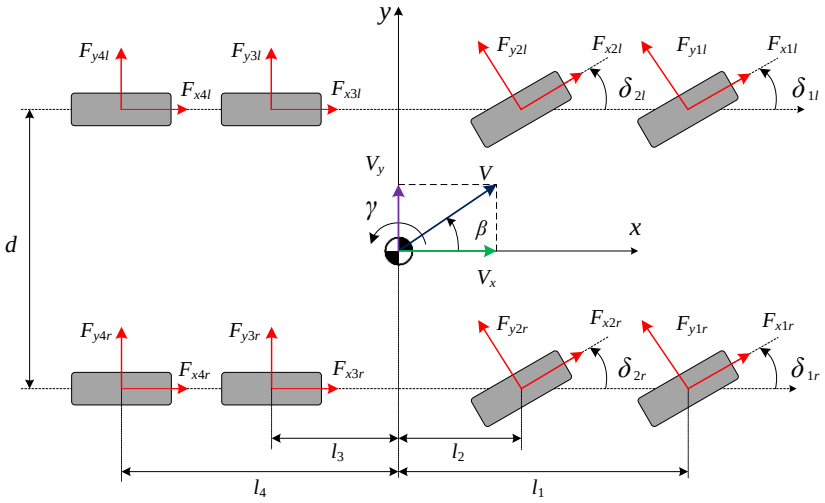

Figure 6. 11-DOF planar vehicle model

The 11-DOF vehicle model (Figure 7) comprises the heave, pitching, and rolling motions of the body of the vehicle and the vertical movements of each of its wheels [70]. The input to this model is the road's vertical profile elevation. Hudha *et al.* [63] considered the firing reaction force at the weapons' platform of a light armoured vehicle as an additional disturbance.

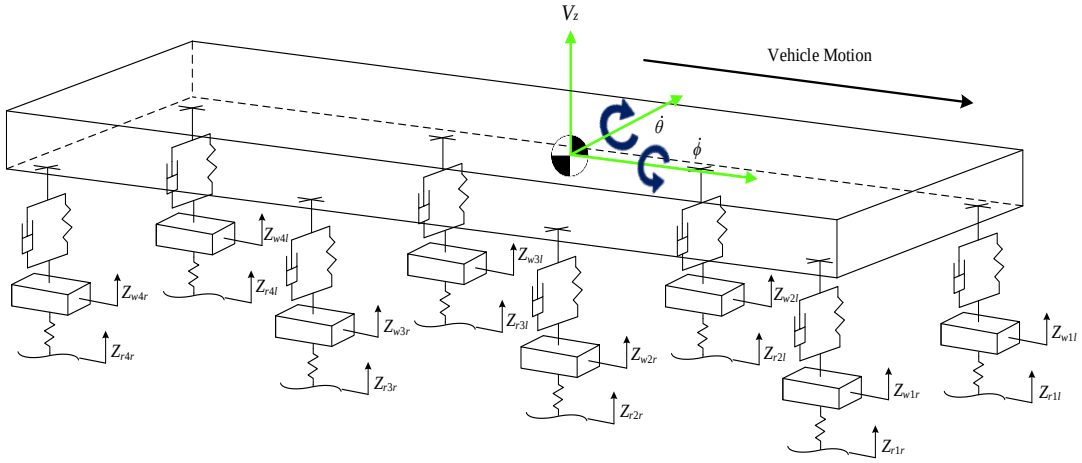

Figure 7. 11-DOF vehicle ride model

2.2.3 22-DOF vehicle model

The 22-DOF vehicle model, depicted in Figure 8, is comprised of the translational motions in the longitudinal, lateral, and vertical directions and the yawing, rolling, and pitching motions of the body of the vehicle, as well as the vertical and rotating movements of each wheel. Similar models were used by Liu and Zhang [55], Zhao and Zhang [65], and Zhifu *et al.* [66].

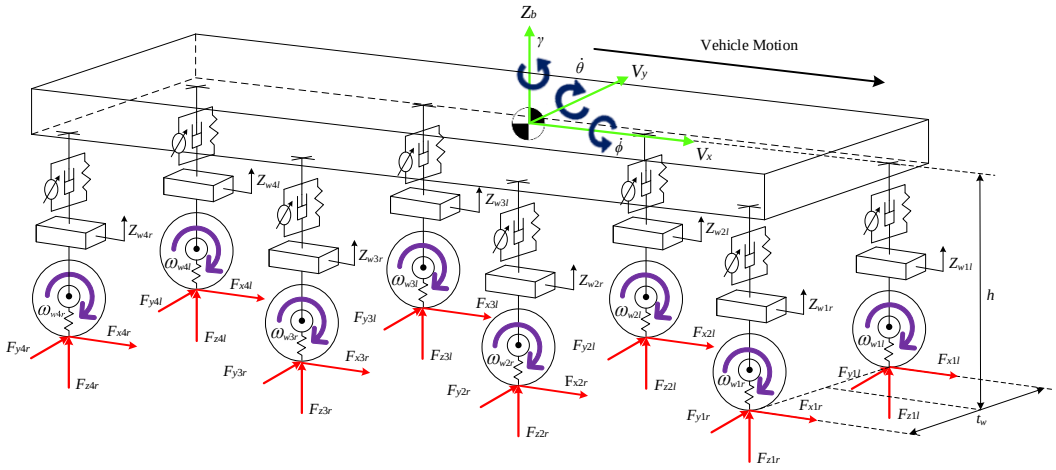

Figure 8. 22-DOF vehicle model

The inputs in the 22-DOF model were the steering angles, driving/braking wheel torques, and road vertical profile elevation. The steering angles inputted for the steerable axles on both sides of the body of the vehicle were the same for each axle. The tyres are considered to be in contact with the road all the time. The tyre longitudinal, lateral, and vertical forces are denoted by F_{xij}, F_{yij}, and F_{zij}, respectively. The rolling and pitching angles and the yawing velocity are represented as ϕ, θ, and γ, respectively. The Z_{wij} is the displacement of the wheel's mass, while ω_{wij} is its rotational speed.

3. TYRE MODELS

A tyre model provides equations with which to determine the TFD in longitudinal and lateral directions. There are two types of tyre models: analytical and empirical. A tyre model comprises three inputs, namely, longitudinal slip ratio, slip angle, and tyre vertical force.

3.1 Dugoff's Tyre Model

Dugoff's tyre model is an analytical tyre model that was used in previous works on MAV's stability control systems [15, 32, 43]. This model assumes that the tyre contact patch has a uniform vertical pressure distribution [71]. It has a few parameters, namely, longitudinal stiffness, lateral stiffness, and tyre-road friction coefficient [72, 73]. It allows for the computation of tyre forces in the longitudinal and lateral directions during simultaneous acceleration/braking and cornering [74]. These tyre forces are more directly linked to the tyre-road friction coefficient. These forces can be given as:

$$F_{xij} = C_\sigma \frac{\sigma_{xij}}{1-\sigma_{xij}} f(\lambda) \tag{5}$$

$$F_{yij} = -C_\alpha \frac{\tan \alpha_{ij}}{1-\sigma_{xij}} f(\lambda) \tag{6}$$

where, the lateral stiffness of a tyre is denoted as C_α and its longitudinal stiffness is denoted as C_σ. The parameter λ was defined as follows:

$$\lambda = \frac{\mu F_{zij}\left(1-\sigma_{xij}\right)}{2\sqrt{\left(C_\sigma \sigma_{xij}\right)^2 + \left(C_\alpha \tan \alpha_{ij}\right)^2}} \tag{7}$$

and

$$f(\lambda) = \begin{cases} (2-\lambda)\lambda & , \quad if\ \lambda < 1 \\ 1 & , \quad \text{otherwise} \end{cases} \tag{8}$$

where, μ is the road coefficient of friction and λ is a nondimensional variable.

3.2 Magic Formula Tyre Model

An example of the empirical tyre model is the Magic Formula tyre model [75]. Previous studies have used this model for MAVs [76–78]. This tyre model can determine the longitudinal and lateral forces on the tyre, as well as the alignment moment [79] and is more accurate than Dugoff's tyre model but requires more parameters. The mathematical equation of this model is expressed as:

$$y(x) = d \sin\{c \arctan[bx - e(bx - \arctan(bx))]\} \tag{9}$$

where, y is either the TFD in the longitudinal or lateral direction in a pure slip condition and x is the longitudinal slip ratio or slip angle of a tyre. Meanwhile, b, c, d, and e are the tyre parameters that were derived from tyre testing data.

4. STANDALONE CONTROL SYSTEMS (SCSS) FOR VEHICLES WITH MORE THAN TWO AXLES

Standalone control systems (SCSs) can be categorised into steering, driving/braking, and suspension control systems. The major goal of these control systems is to enhance the driving/braking performance, stability, manoeuvrability, and/or ride comfort of a vehicle. This section reviews previous works on SCSs. Table 3 lists the types of SCSs, control strategies, number of axles, and vehicle configurations that have been examined.

Table 3. Standalone control systems (SCSs) for multi-axle vehicles (MAVs)

Standalone Control System (SCSs)	Control Strategy	No. of Axles	Actuation Layout	References
Steering	LQR	3	6WS	[17]
	LQR-I	3	6WS	[22]
	MFVS	3	4WS	[20]

Table 3. (cont.)

Standalone Control System (SCSs)	Control Strategy	No. of Axles	Actuation Layout	References
Steering	AISMC	4	8WS	[80]
	MPC	5	10WS	[43]
	LQR	5	10WS	[57]
	SMC-STC	6	12WS	[81]
Driving/Braking	PI-SMC	3	6WID	[20, 96]
	I-SMC and PID	3	6WID	[35]
	SMC	3	6WID/B	[40, 84, 85, 97]
	PID	4	8WID/B	[68]
	SMC	4	8WID/B	[4, 65, 69, 86]
	F-SMC	4	8WID/B	[3]
	SMC	4	8WID/B	[87]
	ISMC	4	6WID/B + 2AMT	[88]
	PID	4	8WID/B	[48]
	LQR	4	8WID/B	[14]
Suspension	FLC	3	SAS	[89]
	LQG	3	SAS	[90]
	FLC and SH	4	SAS	[6]
	ADRC	3	AS	[5]
	FLC	3	AS	[27]
	FLC-PID	3	AS	[91]
	SA	4	AS	[63]

4.1 Steering Control

An active steering control (ASC) system is a type of SCS that enhances the manoeuvrability and stability of a vehicle. Studies have been carried out on ASC strategies for two-axle vehicles. Active steering control (ASC) strategies have also been considered for MAVs. An *et al.* [17] studied a linear quadratic regulator (LQR) control method for a vehicle with six-wheel steering (6WS) to improve its manoeuvrability. The vehicle yaw velocity and sideslip angle were controlled to match the desired vehicle model, whereas the target yaw velocity and sideslip angle were provided by assuming it was a 2-DOF model. The simulation that was performed using an 18-DOF vehicle model for the J-turn test demonstrated that the control system achieved a smaller turning radius and better stability compared to a passive vehicle. The simulation result was confirmed when an experiment was conducted on a scaled-down 6WS vehicle. In another study, similar to the one conducted by An *et al.* [17], an LQR controller was designed with integral control (LQR-I) for a 6WS vehicle to achieve improved manoeuvrability by coordinating the steering angles [22]. This control strategy used LQR-I and an estimator to achieve both the target yaw velocity and a sideslip angle of zero. The evaluation of the control performance through vehicle handling manoeuvres using an 18-DOF vehicle model showed improvement compared to the results obtained by Huh *et al.* [38] and vehicles with ASC at the first axle.

Kang *et al.* [20] designed a model-following variable structure (MFVS) controller to regulate the steer angles of the first and last axles of a vehicle with three axles. This controller uses feedback and feedforward controllers to improve the steer characteristics of an uncertain and nonlinear vehicle model. The controller can improve the steering characteristics on different road conditions compared to vehicles with active front steer and front and rear wheels with fixed control laws. Ahmed *et al.* [80] proposed an ASC at the third and fourth axles of an eight-wheel vehicle to enhance its lateral stability in rough terrain by combining it with an adaptive integral sliding mode controller (AISMC). An AISMC is used to design controllers with disturbance resistance and to reduce lateral displacement error, sideslip angle, and yaw velocity. A simulation was used to assess the performance of the AISMC and LQR during a double-lane change manoeuvre. The AIMSC controller showed better vehicle manoeuvrability and stability than the LQR.

The steering angles were optimised using an LQR with adaptive weighting. The findings showed that this controller outperformed an LQR with a constant weighting matrix with regard to driver steering effort and yaw velocity. Xu *et al.* [81] used the sliding mode control (SMC) and super-twisting control (STC) approaches to regulate the steer angles of the last four axles to enhance the trajectory tracking capability at low velocities and vehicle stability at high velocities for 12WS vehicles. The approach of Xu *et al.* [81] outperformed the LQR and SMC approaches in improving path tracking and vehicle stability.

4.2 Driving or Braking Control

Longitudinal vehicle dynamics is the study of vehicle dynamics in a longitudinal direction. Longitudinal vehicle dynamics focusses on acceleration and braking performance. Longitudinal vehicle control is the control of the vehicle dynamics in a longitudinal direction during acceleration and braking. For example, the traction control system regulates the tyre's longitudinal slip ratio during acceleration to increase the traction between the tyre and the road. Meanwhile, an antilock braking system (ABS) regulates the longitudinal slip ratio to prevent wheel lock-up. This system reduces the stopping distance and maintains vehicle steerability. The direct yaw moment control (DYC) uses the yaw moment produced by the difference between the tyre driving/braking forces on both sides of the vehicle body to turn the vehicle. Next, the TFD algorithm distributes this desired yaw moment to the driving/braking tyre forces. Kang *et al.* [24] designed a skid-steering controller using a six-wheel independent drive (6WID) to increase the stability and trajectory-tracking capability of the vehicle. The system consisted of path tracking, velocity, and vehicle stability controllers. A proportional-integral (PI) controller was designed to follow the target velocity. The vehicle stability controller employed an SMC to increase the vehicle's handling performance, whereas the path tracking controller used the optimal finite preview control method to follow the target path. Simulations and experiments were performed to demonstrate that the controllers were capable of enhancing the stability and trajectory tracking of the vehicle.

Similarly, Zhang *et al.* [35] developed a skid-steering controller for vehicles using a 6WID to increase the stability and manoeuvrability of the vehicles. An integral sliding mode control (I-SMC) computed the longitudinal force of the target vehicle based on the longitudinal velocity error. A proportional-integral-derivative (PID) controller computed the target yaw moment based on the error between the target and the actual yaw rates. This study used the minimisation of the weighted square sum of the used tyre force usage for the TFD. The experimental test result demonstrated that this controller performed better in terms of manoeuvrability and stability compared to previous papers [13, 82]. Nah *et al.* [40] developed a torque distribution controller for skid-steering vehicles that uses a six-wheel independent driving/braking (6WID/B) to improve the manoeuvrability of the vehicle on uneven roads. SMC was utilised to trace the target longitudinal speed profile and target yaw velocity. The friction circle estimation determines the target wheel torque. The results of the simulation demonstrated that the SMC, when combined with friction circle estimation, may enhance vehicle manoeuvrability over terrains better than a proportional distribution method.

Li *et al.* [93] studied a coordinated DYC and ABS for 6WID/B vehicles to increase vehicle stability and reduce the braking distance. Compared with the previous study [93], Lu *et al.* [84] used the same vehicle configuration and coordinated DYC and ABS, with a focus not only on increasing vehicle manoeuvrability and stability but also on reducing the propensity of rollover. The likelihood of the vehicle undergoing rollover was provided by the load transfer ratio (LTR), which is defined as the difference between the tyre vertical forces on both sides of the vehicle divided by the total vehicle weight. A friction estimation approach was utilised for the road friction coefficient estimation. An optimal longitudinal slip ratio was determined using this estimated coefficient of friction and the Burckhardt model. This optimal slip ratio was used as the desired slip ratio for the ABS, which was tracked using the SMC. A DYC was employed to enable independent braking control and to generate yaw moment, thereby enhancing vehicle stability and the propensity for rollover. Hardware-in-loop (HIL) experiments were conducted. The results revealed that the controller was capable of keeping both the vehicle yaw rate and roll angle within safe limits. Zheng *et al.* [85] used a similar approach, but with a different mathematical equation for the LTR.

Ali *et al.* [68] designed a DYC system to prevent rollover in an eight-wheel independent driving/braking (8WID/B) vehicle. The desired longitudinal force of the vehicle was calculated by considering the longitudinal acceleration command from the driver and the longitudinal deceleration generated by a potential field function. The target yaw moment, based on the error between the target and actual yaw rates, was determined by a PID controller. An optimal tyre force distributor provided the wheel torque commands by minimising the square sum of the tyre workload, based on the target longitudinal force and yaw moment of the vehicle. The simulation tests demonstrated that this controller was capable of preventing rollover.

SMC has been used to enhance the manoeuvrability and stability of 8WID/B vehicles [3, 65, 69, 86–88]. There are two approaches for the DYC, one using the optimal TFD method and the other using a heuristic method [13, 65]. The experimental and simulation results of both approaches demonstrated that the use of an optimal TFD for the DYC can improve vehicle stability. Apart from that, a fuzzy-sliding mode control (F-SMC) [3], dual SMC controller [87], and I-SMC [88] can also be used to increase the stability of a vehicle. Other approaches, such as the use of a PID and LQR, have been utilised to determine the desired yaw moment. Ragheb and El-Gindy [48] used a PID controller to calculate the target yaw moment to enhance vehicle stability. Omar and El-Gindy [14] developed an LQR controller to determine the target yawing moment to follow the target path and maintain vehicle stability.

4.3 Suspension Control

Suspension systems are designed to provide good ride comfort and vehicle handling performance. Ride comfort is a fundamental aspect of the suspension system that provides occupants with a smooth and pleasant ride experience. The suspension system also influences the vehicle handling characteristics. Passive suspension systems can be tuned to achieve a balance of good ride comfort and vehicle handling. Semi-active suspension (SAS) or AS systems can further increase the ride comfort and handling performance. An SAS system uses a variable damper to increase ride comfort and

vehicle handling. A magnetorheological (MR) damper, which is an example of a variable damper, uses MR fluid [89, 90]. Variation of the applied magnetic field can alter the viscosity, thereby modifying the damping force. Another type of variable damper is a variable orifice damper [91, 92], where the diameter of the orifice is varied to change the damping force. Various control strategies using SAS dampers have been studied. Li and Nguyen [89] implemented a fuzzy logic control (FLC) for the SAS to increase the ride comfort of a six-wheel vehicle. The damping coefficient was adjusted according to the displacement and velocity measurements.

Also, to improve the ride comfort, Li *et al.* [90] used a linear-quadratic-Gaussian (LQG) controller for SAS. Trikande *et al.* [6] developed a skyhook and FLC for the SAS to enhance road holding and ride comfort when firing a calibre projectile from the gun of an eight-wheel military vehicle. An AS is a kind of suspension system that utilises an electronic control actuator to increase ride comfort and stability performance. Different control strategies using an AS have been investigated in previous studies. Zhu *et al.* [5] designed a controller for a six-wheel rescue vehicle equipped with an AS to increase the vehicle attitude stability. In [27], an AS was developed for the middle axle of a vehicle with three axles to increase vehicle stability. The AS functioned to change the vertical and lateral forces due to road conditions, thereby regulating the yaw moment. FLC was utilised to determine the target actuation force. Bai *et al.* [91] designed an AS with an FLC-PID controller to reduce the heave acceleration of vehicles. Hudha *et al.* [63] developed a stability augmentation system using an AS for an eight-wheel military vehicle to enhance ride comfort under disturbances caused by road irregularities and turret reaction forces.

5. INTEGRATED CONTROL SYSTEMS (ICSS) FOR VEHICLES WITH MORE THAN TWO AXLES

As discussed in the preceding section, the performance of SCSs is limited and can be further enhanced through ICSs. Integrated control systems (ICSs) are categorised into steering and driving/braking control, suspension and driving/braking control, and steering and suspension control systems. Table 4 depicts the various categories of ICSs, control strategies, number of axles, and vehicle configurations.

Table 4. Integrated control systems (ICSs) for multi-axle vehicles (MAVs)

Integrated Control Systems (ICSs)	Control Strategy	No. of Axles	Actuation Layout		References
Steering and Driving/ Braking			Steering	Driving/ Braking	
	LTV-MPC	3	6WS	6WID/B	[31]
	MFAC, FLC, and PID	3	4WS	6WID/B	[82]
	MFPC	3	2WS	6WID/B	[99]
	SMC	3	4WS	4WID/ 6WIB	[58]
	I-SMC	3	6WIS	6WID/B	[15]
	SMC and PID	3	6WIS	6WID/B	[26]
	SMC and PID	3	4WS	6WID	[7]
	SMC and PID	3	6WS	6WID/B	[42]
	SMC and PID	4	4WS	8WID/B	[53]
	SMC	4	8WS	8WID/B	[100]
	SMC	4	4WS	8WID/B	[51]
	PID	4	4WS	8WID/B	[8]
	PI	4	2WS	8WID/B	[101]
	LQR	4	2WS	8WID/B	[102]
	LPV H_∞	4	8WS	8WID/B	[9]
Suspension and Driving/ Braking			Suspension	Driving/ Braking	
	SMC-PID	3	AS	6WID/B	[10]
	SMC	3	SAS	6WID	[11]
Steering and Suspension			Steering	Suspension	
	SMC and H_∞	3	6WS	AS	[103]
	SMC and LQR	3	6WS	AS	[12]

5.1 Integrated Steering and Driving or Braking Control

The integration of the steering and driving/braking control systems has been proven to enhance vehicle stability. This integration utilises the available friction force to improve the limited performance of SCSs. Numerous works have investigated the combination of the steering and driving/braking controls for MAVs. Dong *et al.* [31] designed a linear time-varying model predictive controller (LTV-MPC) to coordinate the ASC and DYC of 6WS and 6WID/B vehicles. Jiang *et al.* [82] developed a control system that combined the steer angle control of the first and third axles, DYC, and speed control for a 6WID/B unmanned ground vehicle with an adjustable wheelbase to enhance the heading angle tracking under low-speed conditions [99]. A model-free adaptive control (MFAC), FLC, and PID controller were utilised to compute the reference steer angle, direct yaw moment, and longitudinal vehicle force, respectively. In another study by Jiang *et al.* [104], a path-following controller for a 6WID/B vehicle with an ASC at the first axle was designed using a model-free predictive control (MFPC) method to enhance vehicle stability at high speeds.

SMC is a popular control strategy used to enhance vehicle stability for both three- and four-axle vehicles [7, 100]. Liu *et al.* [69] designed an SMC to control the speed of a three-axle electric bus using an independent drive at the last two axles of a 6WIB and the ASC strategy at the rear axle while employing the estimated tyre vertical forces to enhance the vehicle stability. Du *et al.* [15] investigated the coordinated control of six-wheel independent steering (6WIS) and 6WID/B vehicles to increase vehicle stability and trajectory tracking performance. The trajectory tracking controller used three SMC controllers to follow the target longitudinal and lateral velocities and target yaw rate. Nah *et al.* [26] designed a controller for 6WIS and 6WID/B vehicles to improve vehicle manoeuvrability in case of fault-tolerant driving. The PID and SMC controllers were developed to determine the target longitudinal vehicle force and yaw moment, respectively. Kim *et al.* [42] employed a PID as the speed controller and the SMC as the vehicle stability controller to compute the direct yaw moment.

An approach similar to the work by Kim *et al.* [42] was proposed for a vehicle with steering control at the first and second axles of an 8WID/B vehicle [53]. Zhang *et al.* [100] proposed an ICS that coordinates the differential braking and ASC at the second, third, and fourth axles to enhance roll and yaw stability. SMC was utilised to determine the target lateral force of a vehicle and its yaw moment. The proposed ICS provided better stability than a standalone differential braking system and ASC. Chen *et al.* [51] designed a coordinated control of the ASC at the first and second axles and DYC of an 8WID/B to enhance vehicle stability. Sliding mode control (SMC) was developed to determine the desired longitudinal and lateral vehicle forces and yaw moment by tracking its velocity profile, sideslip angle, and yaw velocity.

Various control strategies, including PID, LQR, and linear parameter varying H-infinity (LPV-H∞) controllers, have been implemented in the integrated steering and driving/braking control for four-axle vehicles. Li *et al.* [8] employed a PID controller to determine the target longitudinal force for the speed controller and the target direct yaw moment for the yaw rate controller of a vehicle. Tan *et al.* [101] designed a coordinated control system, including the ASC at the fourth axle and DYC, to improve path tracking and vehicle stability. Proportional-integral (PI) controllers were utilised to compute the target drive torque and steering angle. To improve vehicle stability, Luo *et al.* [102] used an LQR controller to determine the target steer angle at the fourth axle and the target direct yaw moment. D'Urso and El-Gindy [9] proposed the coordinated control of an ASC at the third and fourth axles of an 8WID/B vehicle to enhance vehicle stability and decrease the turning radius. An LPV-H_∞ controller was used to compute the steering angle at the fourth axle and the direct yaw moment.

5.2 Integrated Suspension and Driving or Braking Control

The incorporation of an AS or SAS system with the driving/braking control is effective in achieving both vehicle stability and comfort. For instance, to increase the stability of a vehicle, the integration of the AS or SAS with a DYC is known to provide better performance compared to using a DYC alone. When the DYC and steering systems are integrated, aggressive driving/braking and steering may lead to unwanted pitching and rolling motions. These motions can be reduced by using an AS or SAS system to enhance ride comfort. Li *et al.* [11] designed a controller that integrated the yaw motion and attitude controllers for vehicles with an SAS and 6WID to enhance vehicle stability. The yaw motion controller used an SMC to compute the target yaw moment, while the attitude controller used an SMC to calculate the target roll and pitch moments and vertical force. The yaw motion and attitude controllers give better stability compared to the use of a yaw motion controller alone. Chen *et al.* [10] proposed a controller for integrated AS and 6WID/B vehicles with a variable wheelbase to improve vehicle pitch stability. This controller utilised an SMC-PID with an extended state observer control (ESO) to control the AS. The ESO was used to estimate the disturbance of the vehicle, while the SMC-PID was used to adhere to the targeted pitch angle.

5.3 Integrated Steering and Suspension Control

Another type of system that can improve vehicle stability and ride comfort performance is an integrated steering and suspension system. Zhao *et al.* [103] studied a coordination control system integrating AS and 6WS to enhance vehicle stability and comfort. This system employs an H_∞ controller for the steering mechanism and SMC for AS. The root mean square values of the rolling angle, rolling acceleration, and yawing acceleration demonstrated significant improvements with the proposed control method. In a similar approach, Chen *et al.* [12] designed a coordinated AS and 6WS controller to increase ride comfort and vehicle stability. The controller used an SMC to trace the sideslip angle and yaw velocity of the target vehicle, while an LQR controller was designed for the AS to improve the heave, pitching, and rolling motions

of the body of the vehicle. The coordination of active steering and AS provides a lower rolling angle, rolling acceleration, and yawing acceleration.

6. OPTIMAL TYRE FORCE DISTRIBUTION (TFD)

The optimal TFD determines how much longitudinal and lateral force at the tyres must be generated to attain the target longitudinal and lateral vehicle forces and yaw moment. These vehicle forces and moments may be computed by the controller for vehicle stability [106] or collision avoidance [107]. Table 5 shows the objective function, number of axles, actuator layout, and solution method for different optimal TFD methods.

Table 5. Optimal tyre force distribution (TFD) for 2-, 3-, and 4-axle vehicles

Description	Objective Function	No. of Axles	Actuation Layout		Solution	Ref.
			Steering	Driving/ Braking		
Minimisation of the square sum of tyre workload	$J = \sum_{i=1}^{4} \frac{X_i^2 + Y_i^2}{Z_i^2}$	2	4WIS	4WID/B	LES	[108]
Minimisation of the weighted square sum of tyre workload	$J = \sum_{i=1}^{4} w_i \frac{X_i^2 + Y_i^2}{Z_i^2}$	2	4WIS	4WID/B	LES	[115, 125]
Minimisation of the maximum tyre workload	$J = \max_i \frac{X_i^2 + Y_i^2}{Z_i^2}$	2	4WS	4WID/B	GSM & AlS	[107, 116]
Minimisation of the equalised tyre force usage	$J = \frac{\sqrt{X_i^2 + Y_i^2}}{\mu_i Z_i}$	2	4WIS	4WID/B	SQP	[113]
			4WS	4WID/B	CVX	[114]
Minimisation of the square sum of tyre workload	$J = \sum_{i=1}^{6} \frac{X_i^2 + Y_i^2}{Z_i^2}$	3	6WS	6WID/B	LM	[115]
Minimisation of the weighted square sum of tyre force usage	$J = \sum_{i=1}^{2} \frac{w_{xi} X_i^2 + w_{yi} Y_i^2}{(\mu_i Z_i)^2} + \sum_{i=3}^{6} \frac{w_{xi} X_i^2}{(\mu_i Z_i)^2}$	3	6WS	6WID/B	LES	[42]
Minimisation of the weighted square sum of tyre workload	$J = \sum_{i=1}^{6} w_i \frac{X_i^2}{Z_i^2}$	3	Skid Steering	6WID	LES	[11, 20]
Minimisation of the weighted square sum of tyre force usage	$J = \sum_{i=1}^{6} w_i \left(\frac{X_i}{\mu_i Z_i}\right)^2$	3	Skid Steering	6WID	ASM	[94]
			6WIS	6WID/B	LES	[26]
Minimisation of the addition of the square sum of tyre force usage and energy dissipation	$J = \sum_{i=1}^{6} \frac{X_i^2 + Y_i^2}{(\mu_i Z_i)^2} + \sum_{i=1}^{6} (V_{sxi}^2 X_i^2 + V_{syi}^2 Y_i^2)$	3	6WIS	6WID/B	QP	[15]
Minimisation of the addition of the square sum of the difference between longitudinal tyre force and the maximum available tyre force as well as the square sum of the difference between the longitudinal tyre force and the desired longitudinal vehicle force	$J = \sum_{i=1}^{8} (X_i - \mu_i Z_i)^2 + \left[\sum_{i=1}^{8} X_i - F_{xd}\right]^2$	4	4WS	8WID/B	SQP	[55]
Minimisation of the weighted square sum of tyre force usage	$J = \sum_{i=1}^{8} w_{xi} \left(\frac{X_i}{\mu_i Z_i}\right)^2$	4	4WS	8WID/B	SQP	[13]
			4WS	8WID/B	WLS	[46]
			4WS	8WID/B	LES	[53]
Minimisation of the square sum of tyre force usage	$J = \sum_{i=1}^{8} \left(\frac{X_i}{\mu_i Z_i}\right)^2$	4	4WS	8WID/B	WLS	[3]
Minimisation of the weighted square sum of tyre workload	$J = \sum_{i=1}^{8} w_i \frac{X_i^2 + Y_i^2}{Z_i^2}$	4	4WS	8WID/B	LES	[14]

Note: w_i: Weighting Coefficient, w_{xi}: Weighting Coefficient Longitudinal Direction, w_{yi}: Weighting Coefficient Lateral Direction, F_{xd}: Desired Longitudinal Vehicle Force, V_{sxi}: Tyre Longitudinal Slip Speed, V_{syi}: Tyre Lateral Slip Speed, LES: Linear Equation System, GSM: Golden Section Method, AlS: Algebraic Solution, SQP: Sequential Quadratic Programming, LM: Lagrange Multipliers, ASM: Active Set Method, and WLS: Weighted Least Square.

6.1 Tyre Workload and Tyre Force Usage

In an optimal TFD, the maximum tyre workload or tyre force of the tyres is reduced to avoid tyre force saturation. The tyre workload is the vector sum of the longitudinal and lateral tyre forces divided by the tyre's vertical load [116]. Mathematically, it can be given as [112]:

$$W_i = \frac{\sqrt{X_i^2 + Y_i^2}}{Z_i} \tag{10}$$

where, X_i is the longitudinal, Y_i is the lateral, and Z_i is the vertical forces acting on the tyre, respectively.

The tyre force usage is the vector sum of the longitudinal and lateral forces on the tyre divided by the maximum available tyre force [117]. The tyre force usage, also known as the friction usage [114], μ rate [113], and tyre workload rate [118], can be written in mathematical form as:

$$\eta_i = \frac{\sqrt{X_i^2 + Y_i^2}}{\mu_i Z_i} \tag{11}$$

where, μ_i is the road coefficient of friction of the tyre i.

According to the friction circle theory, the tyre force will not be saturated if the value of the tyre workload is less than the value of the friction coefficient [119]. Tyre force saturation will not occur if the tyre force usage is <1 [120]. If the tyre workload approaches the friction coefficient or the tyre force usage approaches 1, the vehicle will be unable to generate additional tyre longitudinal and lateral forces when required by the stability controller or collision avoidance controller. Therefore, the motion of the vehicle may become unstable.

6.2 Optimisation Problems and Solutions

This section describes the optimisation problems and solution methods for an optimal TFD. Different axle numbers and actuation layouts were considered in this paper. The vehicles were categorised as having two axles and more than two axles. Two-axle vehicles, which are the most studied for optimal TFD, are usually assumed to be a combination of a 4WID/B with either a 4WS or 4WIS. For vehicles with three axles, the actuation layouts that are commonly found in the literature are a combination of 6WID/B with 6WS or 6WIS. There are considerable studies on 8WID/B with 4WS for four-axle vehicles. A three-axle vehicle with skid steering will also be discussed in this section.

6.2.1 Vehicle with two axles

An optimal TFD for vehicles with two axles is more commonly studied compared to vehicles with more than two axles. Mokhiamar and Abe [108] proposed the square sum minimisation of tyre workload for 4WIS and 4WID/B distributions. Later, Mokhiamar and Abe [110] extended the optimisation problem to a weighted square sum minimisation with the same actuation layout and LES as a solution method. Nishihara and Higashino [112] proposed a minimax optimisation of tyre workload for 4WS and 4WID/B vehicles, which used the golden section approach to determine the optimal direct yaw moment. Later, Nishihara [111] conducted a comparative study of different optimisation methods. The comparison was made using a contour plot of the maximum tyre workload on a longitudinal-lateral acceleration plane. In the study, the combination of a 4WID/B force distribution with either a 4WS or 4WIS was assumed. The results showed that the envelopes of maximum tyre workload given by the minimax optimisation were considerably larger than those given by the square sum minimisation method. In the proposed two-stage square sum minimisation method, the ordinary square sum was determined in the first stage. In the next stage, the vertical forces on the tyre were determined using Eq. (12):

$$Z_{i,new} = \frac{Z_i}{\sqrt{W_i}} \tag{12}$$

where, Z_i and W_i are the vertical forces on the tyre and tyre workload, respectively, determined in the first stage. This modified approach achieved larger envelopes of the maximum tyre workload compared to those given by the square sum minimisation approach. Therefore, this modified approach achieves better vehicle manoeuvrability compared to the ordinary square sum minimisation approach. Ono *et al.* [113] solved the optimisation problem by utilising sequential quadratic programming (SQP) to achieve the minimum equalised tyre force usage between the four tyres while taking into consideration a vehicle with 4WIS and 4WID/B. Park and Gerdes [114] investigated the minimisation of the equalised tyre force usage between the four tyres of a 4WS vehicle with a 4WID/B actuation layout. The solution to this convex optimisation problem was calculated offline by CVX, a software for solving convex programmes [121].

6.2.2 Vehicle with more than two axles

The optimal TFD has also been studied for vehicles with more than two axles. Kim *et al.* [115] utilised the square sum minimisation of tyre workload for a 6WS vehicle with a 6WID/B system to allocate the target vehicle forces and target yaw moment to the target tyre longitudinal and lateral forces. The optimisation problem was solved by the Lagrange multipliers method [122], and the effects of the controller were demonstrated using TruckSim software. Kim *et al.* [42] studied the weighted square sum minimisation of tyre force usage for a 6WS vehicle with 6WID/B and solved the problem using the LES. The proposed approach yielded better vehicle stability than DYC.

Skid steering changes the direction of a vehicle by using DYC [123]. Kang *et al.* [24] designed an unmanned ground vehicle with skid steering using a 6WID force distribution and used an LES to solve the weighted square sum minimisation of the tyre workload. The optimal TFD with slip control achieved better trajectory tracking performance compared to the force distribution without slip control. Li *et al.* [11] used the same objective function for the TFD for 6WID and SAS to improve vehicle stability. Zhang *et al.* [35] minimised the weighted square sum of the tyre force usage of a 6WID vehicle and solved the optimisation problem using an active set method. The experiments demonstrated that their method performed better in terms of handling and trajectory tracking compared to the methods proposed by [69] and [92]. Also, by minimising the weighted square sum of the tyre force usage, Nah *et al.* [26] investigated a fault-tolerant driving control system for a vehicle with 6WID/B and 6WIS while taking into consideration the failure to steer-by-wire system.

In the literature, the reduction in the energy dissipation caused by the tyre slip during the motion of a vehicle was considered [124]. Du *et al.* [15] studied the optimal TFD by taking into account the tyre force usage and energy dissipation for vehicles with 6WIS and 6WID/B to enhance vehicle stability and reduce energy losses. The solution to minimise the addition of the square sum of the tyre force usage and the energy dissipation was obtained by using the quadratic programming method. Liu *et al.* [16] proposed a controller for a 14WS vehicle while taking into consideration the failure of the steering system of one of the axles to keep the vehicle stable when the trajectory was being tracked. The controller distributed the steer angles of the remaining axles by lowering the tyre workload and energy dissipation.

Multiple studies have examined the optimal TFD for four-axle vehicles. Du *et al.* [55] studied the minimisation of the addition of the square sum of the difference between the longitudinal tyre force and the maximum achievable tyre force and the square of the difference between the sum of the longitudinal tyre forces and the desired longitudinal vehicle force with the SQP method. Kim *et al.* [53] minimised the weighted sum of the squared tyre force usage for vehicles with 4WS and 8WID/B, and this optimisation problem was solved using the LES. The simulation results indicated that the use of the designated drive controller enhanced the vehicle's manoeuvrability when compared to a simple drive controller. Other approaches, such as the SQP [13] and weighted least squares [46], have been utilised to solve the optimisation problem with the same objective function. Zeng *et al.* [3] used the weighted least square method to decrease the square sum of the tyre force usage, which increased vehicle stability and manoeuvrability. Omar and El-Gindy [125] studied the minimisation of the weighted square sum of the tyre workload for vehicles with 8WID/B and 4WS and solved the optimisation problem using the LES.

7. THREE-AXIS TYRE FORCES OPTIMISATION IN MULTI-AXLE VEHICLES (MAVS)

Previous works on MAVs mostly concentrated on determining the optimal distribution of longitudinal and lateral tyre forces. However, studies on two-axle vehicles investigated the optimal distribution of the three-axis tyre forces using two different approaches. In the first approach, the roll stiffness distribution was used to control the vertical tyre forces for vehicles with 4WIS and 4WID/B. Using this approach, Ono *et al.* [126] minimised the equalised tyre force usage among the four tyres and showed that the vehicle achieved better limit performance. The objective function considered in their study can be expressed as:

$$J = \frac{\sqrt{X_i^2 + Y_i^2}}{\mu_i Z_i} \tag{13}$$

In another approach, AS was utilised to control the vertical tyre forces. Luo *et al.* [127] optimised the longitudinal, lateral, and vertical TFD for two-axle vehicles using AS. The optimisation problem was solved using a non-convex method, and the effectiveness of their approach was validated through simulation and experiment by comparing it with three other methods. Their research demonstrated significant enhancements in vehicle stability and ride comfort performance. The following objective function was minimised in their study:

$$J = Var\left(\frac{\sqrt{X_i^2 + Y_i^2}}{\mu_i Z_i}\right) + w_1.avg\left(\frac{\sqrt{X_i^2 + Y_i^2}}{\mu_i Z_i}\right) + w_2.Var\left(\frac{Z_{i,0}}{Z_i}\right) \tag{14}$$

where, w_1 and w_2 are the weights, *Var* is the variance, *avg* is average, and $Zi_{,0}$ is the static load of the tyre *i*. Meanwhile, Nishihara and Sono [128] minimised the maximum tyre workload of four tyres by distributing the roll stiffness and AS control. Equation (15) provides the objective function that was minimised:

$$J = \max_i \frac{X_i^2 + Y_i^2}{(1 - kZ_i)^2 Z_i^2} \tag{15}$$

where *k* is a load-dependent coefficient. The effects of the optimisation of longitudinal and lateral tyre forces, the optimisation of three-axis tyre forces using roll stiffness distribution, and the optimisation of three-axis tyre forces using AS for vehicles with 4WS and 4WID/B were demonstrated through contour plots of the maximum tyre workload. The results showed that the optimisation of three-axis tyre forces using AS produced the largest envelopes on a longitudinal-lateral acceleration plane, indicating the best limit performance of the vehicle among the three optimisation problems. The envelopes produced by the optimisation of three-axis tyre forces using roll stiffness distribution were the second largest among these optimisation problems. For future research, the optimisation of the three-axis tyre forces can be extended to vehicles with more than two axles. By considering the vertical TFD in addition to longitudinal and lateral

TFDs in MAVs, further improvements in vehicle stability and ride comfort can be expected, hence achieving safer MAVs with reduced discomfort.

8. CONCLUSION

This paper presented a review of chassis control for MAVs. Control systems are designed to enhance vehicle stability, trajectory tracking, and ride comfort performances. Chassis control systems can be classified as SCSs and ICSs. Integrated control systems (ICSs), such as the combined steering and wheel torque, suspension and wheel torque, and steering and suspension systems, have been found to provide better performance than SCSs. In an optimal TFD, a controller minimises either the tyre force, tyre workload usage or the dissipation of tyre energy. In this optimal distribution method, the target vehicle forces and yaw moment are allocated to the target tyre forces. To further increase vehicle stability for MAVs, the optimal distribution of the three-axis tyre forces could be an interesting topic for study in the future.

ACKNOWLEDGEMENTS

The first author received a scholarship from the Public Service Department of Malaysia. The authors would like to thank Universiti Teknikal Malaysia Melaka, Malaysia for providing the research facilities.

CONFLICT OF INTEREST

The authors declare that they do not have any conflict of interest.

AUTHORS CONTRIBUTION

M.S.M. Zakaria (Conceptualization, data collection and analysis, manuscript writing and revisions)
A.S.P. Singh (Manuscript revision, editing, and consultations)
M.S.M. Aras (Manuscript revision, editing, and consultations)

REFERENCES

[1] C. Rengaraj, *Integration of Active Chassis Control Systems for Improved Vehicle Handling Performance*, Dissertation, University of Sunderland, 2012.

[2] M. Ahmed, M. El-Gindy, and H. Lang, "Path-following enhancement of an 8×8 combat vehicle using active rear axles steering strategies," *Proceedings of the Institution of Mechanical Engineers, Part K: Journal of Multi-body Dynamics,*, vol. 235, no. 4, pp. 539–552, 2021.

[3] X. Zeng, Y. Li, J. Zhou, D. Song, and X. Li, "Research on yaw stability control of multi-axle electric vehicle with in-wheel motors based on fuzzy sliding mode control," *SAE International Journal of Commercial Vehicles*, vol. 15, no. 3, pp. 259–273, 2022.

[4] Z. Zhang, X. Ma, C. Liu, and S. Wei, "Dual-steering mode based on direct yaw moment control for multi-wheel hub motor driven vehicles: Theoretical design and experimental assessment," *Defence Technology*, vol. 18, no. 1, pp. 49–61, 2022.

[5] J. Zhu, D. Zhao, S. Liu, Z. Zhang, G. Liu, and J. Chang, "Integrated control of spray system and active suspension systems based on model-assisted active disturbance rejection control algorithm," *Mathematics*, vol. 10, no. 18, p. 3391, 2022.

[6] M.W. Trikande, N.K. Karve, R. Anand Raj, V.V. Jagirdar, and R. Vasudevan, "Semi-active vibration control of an 8x8 armored wheeled platform," *Journal of Vibration and Control*, vol. 24, no. 2, pp. 283-302, 2016.

[7] L. Zhang, Y. Jiang, G. Chen, Y. Tang, S. Lu, and X. Gao, "Heading control of variable configuration unmanned ground vehicle using PID-type sliding mode control and steering control based on particle swarm optimisation," *Nonlinear Dynamics*, vol. 111, no. 4, pp. 3361–3378, 2023.

[8] H. Li, J. Li, J. Hu, J. Dong, Z. Hu, L. Xu et al., "Simulation and experiment of distributed drive hybrid multi-axle heavy-duty truck dynamics control algorithm," in *2021 China Automation Congress*, pp. 3497–3502, 2021.

[9] P. D'Urso and M. El-Gindy, "Development of control strategies of a multi-wheeled combat vehicle," *International Journal of Automation and Control*, vol. 12, no. 3, pp. 325–360, 2018.

[10] G. Chen, Y. Jiang, Y. Tang, and X. Xu, "Pitch stability control of variable wheelbase 6WID unmanned ground vehicle considering tire slip energy loss and energy-saving suspension control," *Energy*, vol. 264, p. 126262, 2023.

[11] B. Li, G. Zheng, and Z. Wang, *Attitude control of the vehicle with six in-wheel drive and adaptive hydro pneumatic suspensions*, (No. 2019-01-0456). SAE Technical Paper, 2019.

[12] H. Chen, M.D. Gong, D.X. Zhao, W.B. Liu, and G.Y. Jia, "Coordination control of multi-axis steering and active suspension system for high-mobility emergency rescue vehicles," *Mathematics*, vol. 10, no. 19, p. 3562, 2022.

[13] M.C. Liu, J. Huang, and M. Cao, "Handling stability improvement for a four-axle hybrid electric ground vehicle driven by in-wheel motors," *IEEE Access*, vol. 6, pp. 2668–2682, 2018.

[14] M. Omar and M. El-Gindy, *Direct yaw control based on optimal longitudinal tire forces for 8× 8 combat vehicle*, (No. 2021-01-0261). SAE Technical Paper, 2021.

[15] H. Du, X. Zhu, Q. Liu, T. Ren, and Y. Wang, "Hierarchical coordinated control of multi-axle steering for heavy-duty vehicle based on tire lateral and longitudinal forces optimization," *Proceedings of the Institution of Mechanical Engineers, Part D: Journal of Automobile Engineering*, vol. 238, no. 9, pp. 2727-2740, 2023.

[16] Q. Liu, H. Du, Y. Yu, H. Huang, Y. Wang, and J. Fang, "Research on active safety control for heavy multi-axle vehicles under steering system failure," *Proceedings of the Institution of Mechanical Engineers, Part D: Journal of Automobile Engineering*, p. 09544070231172136., 2023.

[17] S.J. An, K. Yi, G. Jung, K.I. Lee, and Y.W. Kim, "Desired yaw rate and steering control method during cornering for a six-wheeled vehicle," *International Journal of Automotive Technology*, vol. 9, no. 2, pp. 173–181, 2008.

[18] D.E. Williams, "On the equivalent wheelbase of a three-axle vehicle," *Vehicle System Dynamics*, vol. 49, no. 9, pp. 1521–1532, 2011.

[19] Y. Zhang, A. Woo, B. Fidan, and A. Khajepour, "Adaptive yaw control of three-axle road vehicles based on mass, yaw inertia and CG position identification," in *The Canadian Society for Mechanical Engineering International Congress 2018*, pp. 1–6, 2018.

[20] Q. Qu and J. W. Zu, "On steering control of commercial three-axle vehicle," *Journal of Dynamic Systems, Measurement, and Control*, vol. 130, no. 2, p. 021010, 2008.

[21] J. Hu, J. Li, H. Li, J. Dong, Z. Hu, L. Xu et al., "Feedforward and feedback integrated control for handling characteristics adjustment of multi-axle heavy-duty vehicles using independent-drive electric wheels," in *Conference on Vehicular Control and Intelligence*, pp. 1-6, 2021.

[22] B.C. Chen, C.C. Yu and W.F. Hsu, "Steering control of six-wheeled vehicles using linear quadratic regulator techniques," *Proceedings of the Institution of Mechanical Engineers, Part D: Journal of Automobile Engineering*, vol. 221, no. 10, pp. 1231–1240, 2007.

[23] K. Huh, K. Jhang, J. Oh, J. Kim and J. Hong, "Development of a simulation tool for the cornering performance analysis of 6WD/6WS vehicles," *KSME International Journal*, vol. 13, no. 3, pp. 211–220, 1999.

[24] J. Kang, W. Kim, J. Lee, and K. Yi, "Skid steering-based control of a robotic vehicle with six in-wheel drives," *Proceedings of the Institution of Mechanical Engineers, Part D: Journal of Automobile Engineering*, vol. 224, no. 11, pp. 1369–1391, 2010.

[25] W.G. Kim, J.Y. Kang and K. Yi, "Drive control system design for stability and maneuverability of a 6WD/6WS vehicle," *International Journal of Automotive Technology*, vol. 12, no. 1, pp. 67–74, 2011.

[26] J. Nah, W. Kim, K. Yi, D. Lee and J. Lee, "Fault-tolerant driving control of a steer-by-wire system for six-wheel-driving six-wheel-steering vehicles," *Proceedings of the Institution of Mechanical Engineers, Part D: Journal of Automobile Engineering*, vol. 227, no. 4, pp. 506–520, 2013.

[27] A. Soltani, A. Goodarzi, M.H. Shojaeefard and A. Khajepour, "Vehicle dynamics control using an active third-axle system," *Vehicle System Dynamics*, vol. 52, no. 11, pp. 1541–1562, 2014.

[28] S. Wang, J. Zhang and H. Li, "Steering performance simulation of three-axle vehicle with multi-axle dynamic steering," *2008 IEEE Vehicle Power and Propulsion Conference*, pp. 3–7, 2008.

[29] D.E. Williams, "Handling benefits of steering a third axle," *Proceedings of the Institution of Mechanical Engineers, Part D: Journal of Automobile Engineering*, vol. 224, no. 12, pp. 1501–1511, 2010.

[30] M. Yang, X. H. Gao, H. Wang and C. Wang, "Simulation analysis of multi-axle vehicle braking stability based on all-wheel active steering technology," *2010 The 2nd International Conference on Industrial Mechatronics and Automation*, vol. 1, pp. 366–369, 2010.

[31] J. Dong, J. Li, Q. Gao, J. Hu, and Z. Liu, "Optimal coordinated control of active steering and direct yaw moment for distributed-driven electric vehicles," *Control Engineering Practice*, vol. 134, p. 10586, 2023.

[32] A. Jackson, D. Crolla, A. Woodhouse, and M. Parsons, *Improving performance of a 6× 6 off-road vehicle through individual wheel control* , (No. 2002-01-0968). SAE Technical Paper, 2002.

[33] S.H. Kim, D.H. Kim, C.J. Kim, Y.R. Kim, J.Y. Choi, and C.S. Han, "A study on motion control of 6WD/6WS vehicle using optimum tire force distribution method," *International Conference on Control, Automation and Systems 2010*, pp. 1502–1507, 2010.

[34] X. Zeng, G. Li, G. Yin, D. Song, S. Li, and N. Yang, "Model predictive control-based dynamic coordinate strategy for hydraulic hub-motor auxiliary system of a heavy commercial vehicle," *Mechanical Systems and Signal Processing*, vol. 101, pp. 97–120, 2018.

[35] H. Zhang, H. Liang, X. Tao, Y. Ding, B. Yu, and R. Bai, "Driving force distribution and control for maneuverability and stability of a 6WD skid-steering EUGV with independent drive motors," *Applied Sciences*, vol. 11, no. 3, pp. 1–21, 2021.

[36] A. Soltani, A. Goodarzi, M.H. Shojaeefard, and A. Khajepour, "Vehicle dynamics control using an active third-axle system," *Vehicle System Dynamics*, vol. 52, no. 11, pp. 1541–1562, 2014.

[37] S.L. Cho, K.C. Yi, J.H. Lee, and W.S. Yoo, "Manoeuvring speed of a 6×6 autonomous vehicle using a database obtained from multi-body dynamic simulation," *Proceedings of the Institution of Mechanical Engineers, Part D: Journal of Automobile Engineering*, vol. 223, no. 8, pp. 979–985, 2009.

[38] K. Huh, J. Kim, and J. Hong, "Handling and driving characteristics for six-wheeled vehicles," *Proceedings of the Institution of Mechanical Engineers, Part D: Journal of Automobile Engineering*, vol. 214, no. 2, pp. 159–170, 2000.

[39] S.H. Kim, C.J. Kim, and C.S. Han, "Improvement of hill climbing ability for 6WD/6WS vehicle using optimum tire force distribution method," *Journal of the Korea Academia-Industrial cooperation Society*, vol. 12, no. 4, pp. 1523–1531, 2011.

[40] J. Nah, J. Seo, K. Yi, W. Kim, and J. Lee, "Friction circle estimation-based torque distribution control of six-wheeled independent driving vehicles for terrain-driving performance," *Proceedings of the Institution of Mechanical Engineers, Part D: Journal of Automobile Engineering*, vol. 229, no. 11, pp. 1469–1482, 2015.

[41] Y. Ma, X. Li, and J. Zhi, "The Research of Torque distribute strategy for 6-wheel-independent-driving (6WID) electric vehicle," *2014 IEEE Conference and Expo Transportation Electrification Asia-Pacific (ITEC Asia-Pacific)*, pp. 4–8, 2014.

[42] W.G. Kim, K. Yi, and J. Lee, "An optimal traction, braking, and steering coordination strategy for stability and manoeuvrability of a six-wheel drive and six-wheel steer vehicle," *Proceedings of the Institution of Mechanical Engineers, Part D: Journal of Automobile Engineering*, vol. 226, no. 1, pp. 3–22, 2012.

[43] K. Oh, J. Seo, J. Kim, and K. Yi, "An investigation on steering optimisation for minimum turning radius of multi-axle crane based on MPC algorithm," in *International Conference on Control, Automation and Systems (ICCAS 2015)*, pp. 1974–1977, 2015.

[44] W. Wang, J. Li, X. Li, Z. Li, and N. Guo, "Multi-objective collaborative control method for multi-axle distributed vehicle assisted driving," *Applied Sciences*, vol. 13, no. 13, p. 7769, 2023.

[45] Q. Wang, J. Goyal, B. Ayalew, and A. Singh, "Control allocation for multi-axle hub motor driven land vehicles with active steering," in *ASME Design Engineering Technical Conference*, vol. 3, pp. 1–8, 2016.

[46] C. Zhang, Y. Chen, Z. Wang, and C. Wang, "An optimal control allocation strategy for an eight in-wheel-motor drive electric vehicle," in *43rd Annual Conference of the IEEE Industrial Electronics Society*, pp. 109–114, 2017.

[47] R. Zhang, C. Zhang, and M. Liu, "Handling characteristics of a four-axle electric vehicle," in *IEEE Transportation Electrification Conference and Expo, ITEC Asia-Pacific 2014*, pp. 1–6, 2014.

[48] H. Ragheb and M. El-Gindy, "Design of active yaw controller integrated with ABS and TCS for multi-wheeled vehicles," *International Journal of Vehicle Systems Modelling and Testing*, vol. 13, no. 4, pp. 340–357, 2019.

[49] L. Cai, Z. Liao, S. Wei, and J. Li, "Improvement of maneuverability and stability for eight wheel independently driven electric vehicles by direct yaw moment control," *2021 24th International Conference on Electrical Machines and Systems*, pp. 2482–2487, 2021.

[50] K. Bayar and Y.S. Unlusoy, "Steering strategies for multi-axle vehicles," *International Journal of Heavy Vehicle Systems*, vol. 15, no. 2–4, pp. 208–236, 2008.

[51] Y. Chen, C.N. Zhang, and M. Zhang, "Control allocation based on all wheel control in the dynamic control of eight in-wheel motor drive vehicle," in *DEStech Transactions on Engineering and Technology Research*, pp. 78–85, 2017.

[52] V.V. Jagirdar, V.P. Maskar, and M.W. Trikande, "Steering strategy for a multi-axle wheeled vehicles," in *International Conference on Advances in Mechanical, Industrial, Automation and Management Systems*, pp. 164–171, 2017.

[53] W.G. Kim, K. Yi, and J. Lee, "Drive control algorithm for an independent 8 in-wheel motor drive vehicle," *Journal of Mechanical Science and Technology*, vol. 25, no. 6, pp. 1573–1581, 2011.

[54] C. Liu, G. Yang, and J. Li, "Dual-steering control strategy for 8-wheel vehicle driven by hub motor," in *IEEE Vehicle Power and Propulsion Conference, VPPC 2016*, pp. 2–6, 2016.

[55] M.C. Liu and C.N. Zhang, "Development of an optimal control system for longitudinal and lateral stability of an individual eight-wheel-drive electric vehicle," *International Journal of Vehicle Design*, vol. 69, no. 1–4, pp. 132–150, 2015.

[56] J. Ni and J. Hu, "Handling performance control for hybrid 8-wheel-drive vehicle and simulation verification," *Vehicle System Dynamics*, vol. 54, no. 8, pp. 1098–1119, 2016.

[57] K. Oh, J. Seo, and J.W. Han, "LQR-based adaptive steering control algorithm of multi-axle crane for improving driver's steering efficiency and dynamic stability," in *International Conference on Control, Automation and Systems*, pp. 792–796, 2016.

[58] S. Ding, L. Liu, and W.X. Zheng, "Sliding mode direct yaw-moment control design for in-wheel electric vehicles," *IEEE Transactions on Industrial Electronics*, vol. 64, no. 8, pp. 6752–6762, 2017.

[59] Y. Sun and Z. Wu, "Study on steering mobility of multi-axle vehicles with independent braking system," in *IEEE International Conference on Mechatronics and Automation*, pp. 2249–2254, 2018.

[60] Q. Wang, B. Ayalew, and A. Singh, "Control allocation for multi-axle hub motor driven land vehicles," *SAE International Journal of Alternative Powertrains*, vol. 5, no. 2, pp. 338–347, 2016.

[61] L. Li, H. Wang, D. Pi, X. Wang, E. Wang, and Y. Chen, "Research on torque distribution control of high performance distribution drive multi-axle special vehicle," in *2022 6th CAA International Conference on Vehicular Control and Intelligence*, pp. 1-8, 2022.

[62] V.V. Jagirdar, V.P. Maskar, and M.W. Trikande, "Handling simulation and experimentation of an armoured multi-axle vehicle with multi-axle steering," in *Innovative Design and Development Practices in Aerospace and Automotive Engineering. Lecture Notes in Mechanical Engineering*, Springer Singapore, pp. 447–453, 2017.

[63] K. Hudha, H. Jamaluddin, and P.M. Samin, "Disturbance rejection control of a light armoured vehicle using stability augmentation based active suspension system," *International Journal of Heavy Vehicle Systems*, vol. 15, no. 2–4, pp. 152–169, 2008.

[64] M.W. Trikande, V.V. Jagirdar, and M. Sujithkumar, "Modelling and comparison of semi-active control logics for suspension system of 8×8 armoured multi-role military vehicle," *Applied Mechanics and Materials*, vol. 592–594, pp. 2165–2178, 2014.

[65] Y. Zhao and C. Zhang, "Electronic stability control for improving stability for an eight in-wheel motor-independent drive electric vehicle," *Shock and Vibration*, vol. 1, p. 8585670, 2019.

[66] W. Zhifu, W. Yunzhao, G. Zhiqiang, and G. Jian, "Torque distribution control strategy based on dynamic axle load for 8 in-wheel motor drive vehicle," in *Energy Procedia*, vol. 104, pp. 550–555, 2016.

[67] M.C. Liu, C. Zhang, R. Zhang, and Z. Wang, "Research on steady and transient characteristics of 4-axle vehicle handling," in *IEEE Transportation Electrification Conference and Expo, ITEC Asia-Pacific 2014*, pp. 1–6, 2014.

[68] M.A.Ali, C. Kim, S. Kim, A.M. Khan, J. Iqbal, M.Z. Khalil et al., "Lateral acceleration potential field function control for rollover safety of multi-wheel military vehicle with in-wheel-motors," *International Journal of Control, Automation and Systems*, vol. 15, no. 5, pp. 837–847, 2017.

[69] W. Liu, H. He, F. Sun, and J. Lv, "Integrated chassis control for a three-axle electric bus with distributed driving motors and active rear steering system," *Vehicle System Dynamics*, vol. 55, no. 5, pp. 601–625, 2017.

[70] M.W. Trikande and V. Rajamohan, "MR damper characterization for implementation of semi-active suspension control," *Indian Journal of Science and Technology*, vol. 9, no. 30, 2016.

[71] R. Rajamani, *Vehicle Dynamics and Control*, 2nd ed. Minneapolis, 2006.

[72] H. Dugoff, P.S. Fancher, and L. Segel, "Tire Performance Characteristics Affecting Vehicle Response to Steering and Braking Control Inputs," Michigan, 1969.

[73] H. Dugoff, P.S. Fancher, and L. Segel, "An analysis of tire traction properties and their influence on vehicle dynamic performance," *SAE Technical Paper 700377*, pp. 1-25, 1970.

[74] M. Doumiati, A. Charara, A. Victorino, and D. Lechner, *Vehicle Dynamics Estimation using Kalman Filtering*, John Wiley & Sons, 2012.

[75] H. B. Pacejka and E. Bakker, "The Magic Formula Tyre Model," *Int. J. Veh. Mech. Mobil.*, vol. 21, no. S1, pp. 1–18, 1992.

[76] Y. J. Chung, T. C. Lin, and T. Liu, "Analysis and Evaluation of 8x8 4-axle Vehicle with Assisted Steering System," in *IEEE*, 2018, pp. 9–12.

[77] Y. Zhang, A. Khajepour, and M. Ataei, "A universal and reconfigurable stability control methodology for articulated vehicles with any configurations," *IEEE Transactions on Vehicular Technology*, vol. 69, no. 4, pp. 3748–3759, 2020.

[78] L. Jin, D. Tian, Q. Zhang, and J. Wang, "Optimal torque distribution control of multi-axle electric vehicles with in-wheel motors based on DDPG algorithm," *Energies*, vol. 13, no. 6, p. 1331, 2020.

[79] H.B. Pacejka, *Tire and Vehicle Dynamics*, 3rd ed., Elsevier, 2012.

[80] M. Ahmed, M. El-Gindy, and H. Lang, "A novel adaptive-rear axles steering controller for an 8×8 combat vehicle," *Proceedings of the Institution of Mechanical Engineers, Part C: Journal of Mechanical Engineering Science*, vol. 1, no. 14, 2021.

[81] T. Xu, X. Liu, Z. Li, B. Feng, X. Ji, and F. Wu, "A sliding mode control scheme for steering flexibility and stability in all-wheel-steering multi-axle vehicles," *International Journal of Control, Automation and Systems*, vol. 21, no. 6, pp.1926-1938., 2023.

[82] Y. Jiang, X. Xu, and L. Zhang, "Heading tracking of 6WID/4WIS unmanned ground vehicles with variable wheelbase based on model free adaptive control," *Mechanical Systems and Signal Processing*, vol. 159, p. 107715, 2021.

[83] S. Li, J. Zhao, S. Yang, and H. Fan, "Research on a coordinated cornering brake control of three-axle heavy vehicles based on hardware-in-loop test," *IET Intelligent Transport Systems*, vol. 13, no. 5, pp. 905–914, 2019.

[84] Y. Lu, Y. Han, W. Huang, and Y. Wang, "Sliding mode control for overturning prevention and hardware-in-loop experiment of heavy-duty vehicles based on dynamical load transfer ratio prediction," *Proceedings of the Institution of Mechanical Engineers, Part K: Journal of Multi-body Dynamics*, vol. 236, no. 1, pp. 68–83, 2022.

[85] L. Zheng, Y. Lu, H. Li, and J. Zhang, "Anti-rollover control and HIL verification for an independently driven heavy vehicle based on improved LTR," *Machines*, vol. 11, no. 1, p. 117, 2023.

[86] Z. Liao, L. Cai, Q. Yang, and Y. Zhang, "Design of lateral dynamic control objectives for multi-wheeled distributed drive electric vehicles," *Engineering Science and Technology, an International Journal*, vol. 50, p. 101629, 2024.

[87] L. Cai, Z. Liao, S. Wei, and J. Li, "Novel direct yaw moment control of multi-wheel hub motor driven vehicles for improving mobility and stability," *IEEE Transactions on Industry Applications*, vol. 59, no. 1, pp. 591–600, 2023.

[88] Z. Shuai, C. Li, J. Gai, Z. Han, G. Zeng, and G. Zhou, "Coordinated motion and powertrain control of a series-parallel hybrid 8×8 vehicle with electric wheels," *Mechanical Systems and Signal Processing*, vol. 120, pp. 560–583, 2019.

[89] H. Li and V. Nguyen, "Improving ride comfort and road friendliness of heavy truck using semi-active suspension system," *Robotic Systems and Applications*, vol. 3, no. 1, pp. 3-26, 2023.

[90] S. Li, J. Zhao, and Z. Zhang, "Investigation on linear quadratic gaussian control of semi-active suspension for three-axle vehicle," *Journal of Low Frequency Noise, Vibration and Active Control*, vol. 40, no. 3, pp. 1633–1648, 2021.

[91] X. Bai, L. Lu, C. Zhang, and W. Geng, "Research on height adjustment characteristics of heavy vehicle active air suspension based on fuzzy control," *World Electric Vehicle Journal*, vol. 14, no. 8, p. 210, 2023.

[92] Y. Song, H. Shu, X. Chen, and S. Luo, "Direct yaw moment control of four-wheel-drive electrical vehicle based on lateral tyre-road forces and sideslip angle observer," *IET Intelligent Transport Systems*, vol. 13, no. 2, pp. 303–312, 2018.

[93] H. Li, J. Li, J. Hu, B. Cai, L. Xu, and M. Ouyang, "Hardware-in-the-loop simulation of electronic differential moment power steering control strategy for multi-axle vehicle," *2019 3rd Conference on Vehicle Control and Intelligence*, pp. 1–4, 2019.

[94] Z. Zhang, C. Liu, X. Ma, Y. Zhang, and L. Chen, "Driving force coordinated control of an 8×8 in-wheel motor drive vehicle with tire-road friction coefficient identification," *Defence Technology.*, vol. 18, no. 1, pp. 119–132, 2020.

[95] Y.K. Chen, J. He, M. King, Z.X. Feng, and W.H. Zhang, "Comparison of two suspension control strategies for multi-axle heavy truck," *Journal of Central South University*, vol. 20, no. 2, pp. 550–562, 2013.

[96] S.H. Ha, M.S. Seong, and S.B. Choi, "Design and vibration control of military vehicle suspension system using magnetorheological damper and disc spring," *Smart Materials and Structures*, vol. 22, no. 6, p. 0565006, 2013.

[97] B. Gong, X. Guo, S. Hu, and L. Xu, "Ride comfort optimization of a multi-axle heavy motorized wheel dump truck based on virtual and real prototype experiment integrated kriging model," *Advances in Mechanical Engineering*, vol. 7, no. 6, p.1687814015584257, 2015.

[98] K. Kwon, M. Seo, H. Kim, T.H. Lee, J. Lee, and S. Min, "Multi-objective optimisation of hydro-pneumatic suspension with gas–oil emulsion for heavy-duty vehicles," *Vehicle System Dynamics*, vol. 58, no. 7, pp. 1146–1165, 2020.

[99] W.H. Wang, X.J. Xu, H.J. Xu, and F.L. Zhou, "Enhancing lateral dynamic performance of all-terrain vehicles using variable-wheelbase chassis," *Advances in Mechanical Engineering*, vol. 12, no. 5, p. 1687814020917776, 2020.

[100] B. Zhang, C. Zong, G. Chen, Y. Huang, and T. Xu, "A novel integrated stability control based on differential braking and active steering for four-axle trucks," *Chinese Journal of Mechanical Engineering*, vol. 32, no. 12, pp. 1–21, 2019.

[101] S. Tan, Y. Wang, W. Cheng, T. Luo, N. Zhang, S. Li et al., "Cascade direct yaw moment control for an independent eight in-wheel motor-driven autonomous vehicle," *Electronics*, vol. 11, no. 18, p. 2930, 2022.

[102] T. Luo, B. Su, N. Zhang, and S. Tan, "A control allocation strategy of multi-axle unmanned distributed drive vehicle," in *Conference on Artificial Intelligence and Computer Engineering*, pp. 674–679, 2021.

[103] D. Zhao, M. Gong, D. Zhao, W. Liu, and W. Chen, "Active suspension and steering system control of emergency rescue vehicle based on sliding mode dual robust coordination control," *Advances in Mechanical Engineering*, vol. 16, no. 6, p. 16878132241259720, 2024.

[104] Y. Jiang, X. Xu, L. Zhang, and T. Zou, "Model free predictive path tracking control of variable-configuration unmanned ground vehicle," *ISA Transactions*, vol. 129, pp. 485–494, 2022.

[105] L. Zhang, H. Ding, K. Guo, J. Zhang, W. Pan, and Z. Jiang, "Cooperative chassis control system of electric vehicles for agility and stability improvements," *IET Intelligent Transport Systems*, vol. 13, no. 1, pp. 134–140, 2019.

[106] J. Nah and S. Yim, "Vehicle stability control with four-wheel independent braking, drive and steering on in-wheel motor-driven electric vehicles," *Electronics*, vol. 9, no. 11, p. 1934, 2020.

[107] A.S.P. Singh and O. Nishihara, "Minimum resultant vehicle force optimal state feedback control for obstacle avoidance," *IEEE Transactions on Control Systems Technology*, vol. 28, no. 5, pp. 1846–1861, 2020.

[108] O. Mokhiamar and M. Abe, "Effect of an optimum cooperative chassis control from the view point of tire workload," *Society of Automotive Engineers of Japan*, vol. 33, no. 3, pp. 15–20, 2003.

[109] M. Abe and O. Mokhiamar, "An integration of vehicle motion controls for full drive-by-wire vehicle," *Proceedings of the Institution of Mechanical Engineers, Part K: Journal of Multi-body Dynamics*, vol. 221, no. 1, pp. 117–127, 2007.

[110] O. Mokhiamar and M. Abe, "Simultaneous optimal distribution of lateral and longitudinal tire forces for the model following control," *Journal of Dynamic Systems, Measurement, and Control*, vol. 126, no. 4, pp. 753–763, 2004.

[111] O. Nishihara, "Comparison of optimisation schemes for tire force distribution in integrated chassis control," *12th International Symposium on Advanced Vehicle Control*, pp. 409–414, 2014.

[112] O. Nishihara and S. Higashino, "Exact solution to four-wheel independent driving/ braking force distribution and direct yaw-moment optimization with minimax criterion of tire workload," *11th International Symposium on Advanced Vehicle Control*, vol. 12, no. 1, pp. 1–6, 2012.

[113] E. Ono, Y. Hattori, Y. Muragishi, and K. Koibuchi, "Vehicle dynamics integrated control for four-wheel-distributed steering and four-wheel-distributed traction/ braking systems," *Vehicle System Dynamics*, vol. 44, no. 2, pp. 139–151, 2006.

[114] H. Park and J. C. Gerdes, "Optimal tire force allocation for trajectory tracking with an over-actuated vehicle," *2015 IEEE Intelligent Vehicles Symposium (IV)*, pp. 1032–1037, 2015.

[115] D.H. Kim, C.J. Kim, Y.R. Kim, and C.S. Han, "A study on an independent 6WD/6WS of electric vehicle using optimum tire force distribution (Korean version)," *Journal of Institute of Control, Robotics and Systems*, vol. 16, no. 7, pp. 632–638, 2010.

[116] M. Abe, *Vehicle Handling Dynamics Theory and Application*, 2nd ed. Oxford, 2015.

[117] A. Alleyne, "A comparison of alternative obstacle avoidance strategies for vehicle control," *Vehicle System Dynamics*, vol. 27, no. 5–6, pp. 371–392, 1997.

[118] L. Zhang, Z. Zhang, Z. Wang, J. Deng, and D. G. Dorrell, "Chassis coordinated control for full x-by-wire vehicles-A review," *Chinese Journal of Mechanical Engineering*, vol. 34, no. 42, pp. 1–25, 2021.

[119] O. Nishihara and S. Higashino, "Optimum distribution of lateral and traction/ braking forces for energy conservation," *7th International Federation of Automatic Control Symposium on Advances in Automotive Control*, vol. 46, no. 21, pp. 631–636, 2013.

[120] S. Horiuchi, K. Okada, and S. Nohtomi, "Optimum steering and braking control strategies in obstacle avoidance maneuvers," *7th International Symposium on Advanced Vehicle Control AVEC04*, pp. 619–624, 2004.

[121] M. Grant and S. Boyd, *CVX: Matlab Software for Disciplined Convex Programming* | CVX Research, Inc. Version 2.1, 2014.

[122] J.S. Arora, *Introduction to Optimum Design*, 3rd ed. Iowa City: Elsevier Ltd., 2012.

[123] H. Sasaki and M. Abe, "Behavior analysis of skid steer control vehicles," *International Federation of Automatic Control Proceedings Volumes*, vol. 37, no. 22, pp. 709–714, 2004.

[124] Y. Suzuki, Y. Kano, and M. Abe, "A study on tyre force distribution controls for full drive-by-wire electric vehicle," *Vehicle System Dynamics*, vol. 52, no. Sup.1, pp. 235–250, 2014.

[125] M. Omar and M. El Gindy, "Vehicle yaw stability control: Literature review," *International Journal of Vehicle Systems Modelling and Testing*, vol. 16, no. 4, p. 259, 2022.

[126] E. Ono, Y. Hattori, and S. Monzaki, "Improvement in critical performance of vehicle dynamics integrated control by optimal distribution of four wheel tire forces (Japanese)," *Transactions-Society of Automotive Engineers of Japan*, vol. 39, no. 2, pp. 33–38, 2008.

[127] Y. Luo, K. Cao, Y. Xiang, and K. Li, "Vehicle stability and attitude improvement through the coordinated control of longitudinal, lateral, and vertical tyre forces for electric vehicles," *International Journal of Vehicle Design*, vol. 69, pp. 25–49, 2015.

[128] O. Nishihara and K. Sono, "Reduction of tire workload with distribution of normal loads on wheels," in *The Proceedings of Mechanical Engineering Congress, Japan*, p. G1000502, 2015.